Proceedings of The Canadian Society for Mechanical Engineering International Congress 2018
CSME International Congress 2018
May 27-30, 2018, Toronto, On, Canada

Characterization of the electrodes of DEP-based micro-separator

Arash Dalili, Erfan Taatizadeh, Mina Hoorfar
School of Engineering
University of British Columbia
Kelowna, Canada
mina.hoorfar@ubc.ca

Abstract—In recent years, advances in lab-on-a-chip (LOC) devices has led to separation, sorting and manipulation of cells and particles on miniaturized devices. Among the different mechanisms that have been used in this regard, dielectrophoresis (DEP) offers high controllability on the particles, provides high throughput, and is tunable. Due to these advantages, DEP is used in this paper for the design of a micro-separator. To optimize the geometry of such a separator, COMSOL Multiphysics® is used to simulate the electric field with the goal of achieving the highest performance in cell separation. For a DEP-based micro-separator, two inclined rectangle planar electrodes are considered. The effect of the width of each one of these electrodes as well as the gap between them on the DEP force is investigated to find the optimum design.

Keywords- DEP; COMSOL modeling; Optimization, Microfluidics

I. INTRODUCTION

The separation of cells and particles in a micro scale has attracted the attention of researchers in the fields of microfluidics, bio-engineering, biology, chemistry, etc. The researchers are using different methods, which can be categorized into passive and active. The passive methods include micro-filters, micro-devices based on inertial forces, deterministic lateral displacement and the pinched flow fractionation. While the passive operate on their own, the active methods rely on an external force to manipulate the cells or particles, which can lead to more accurate and specific separation. Acoustic, magnetic, optical and electrical forces are among the forces that are used for cell/particle manipulation. The electric force can manipulate charged particles, which is called electrophoresis, or it can manipulate uncharged particles, which is called dielectrophoresis (DEP). DEP has been used by researchers for different applications such as cell patterning [1], trapping [2, 3], focusing [4], enrichment [5], separation [6] and isolation [7, 8]. DEP can separate the cells based on their electrical properties (electrical conductivity and permittivity) and size. Although some studies have used biomarkers to change the electrical properties of the cells [9], in general, DEP is a marker-free method depending on the intrinsic properties of the cells. Eliminating the labeling of the cells and biomarkers makes the preparation for DEP-based separation much faster and cheaper than some other methods such as fluorescence-activated cell sorter (FACS) and magnetic-activated cell sorter (MACS). Another advantage of DEP over other marker-free techniques is its relative ease of fabrication compared to other techniques such as those based on acoustic forces.

Different configureations of electordes such as interdigitated [10], castellated [11], top-bottom paterned [12] and sidewall patterned [13] have been used for DEP-based devices. Among these configurations, planar slanted electrodes are easy to fabricate and operate, and are suitable for continuous cell separation. The slanted electrodes can continuously move the cells laterally toward the target outlet.

To apply an effective DEP force for cell/particle separation, the design needs to be optimized. This optimized design can lead to higher throughput and lower voltage (which means lower joul heating and higher cell viability). In this study, slanted electrodes are chosen and simulation is used to find the optimum width of the electrodes and the gap between them for achieving a maximum DEP force and hence effective cell separation.

II. THEORY OF DIELECTROPHORETIC FORCE

When a particle is in a non-uniform electric field, it is polarized and experiences a force from the electric field. This phenomenon is referred to as DEP. The DEP force can be calculated as:

$$F_{DEP} = 2\pi\varepsilon_m R^3 CM\nabla E^2 \quad (1)$$

where ε_m is the absolute permittivity of the medium, R is the radius of the particle, CM is the Clausius Mossotti factor and E is the electric field. The CM factor depends on the relative permittivity of the particle and medium, and it is the factor that determines the sign of the DEP force as described below:

$$CM = \frac{\varepsilon_p - \varepsilon_m}{\varepsilon_p + 2\varepsilon_m} \quad (2)$$

Based on the sign of the CM factor, there are two categories of DEP: negative dielectrophoresis (nDEP) and positive dielectrophoresis (pDEP). The pDEP happens when the particles are more polarizable than the medium and the DEP force on the particles is towards the highest intensity of the electric field regions. On the other hand, the higher polarizability of the medium in comparison to the particle generates an nDEP effect,

pushing the particles towards the regions with the lowest intensity of gradient of the electric field square.

III. COMPUTATIONAL MODELING

The electric current module of COMSOL Multiphysics software have been used for the simulation of our design.

Figure 1 shows the geometry (the cross section along width of the channel) which has been used for studying the effect of DEP on cell separation. The geometry consists of two rectanglar electrodes, which are positioned at the bottom of the microfluidics channel. The channel is 1 mm × 75 µm and height of the electrodes are 100 nm. The width of the electrodes varies from 10 to 200 µm during simulation to investigate the effect of the electrode size on the DEP force.

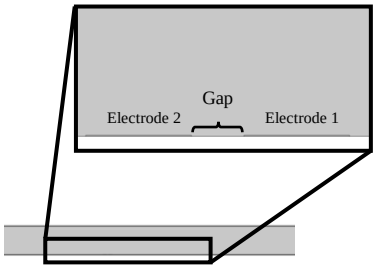

Figure 1. The geometry used for simulation

The minimum feature size that we can fabricate in our clean room is 5 µm. Therefore, this is the minimum gap (see Fig 1) that is used in this study. The simulation has been done for gaps ranging from 5 to 85 µm and electode width ranging from 10 to 300 µm. 1 volt AC electric current with a frequency of 100 kHz is applied to the electrodes and the other boundaries of the channel is assumed to be isolated.

Electrical potential of 1 and -1 voltage were used as boundary conditions for electrode 1 and 2, respectively. In addition, at the interface of the electodes and fluid, continuity boundary condition was assumed. Furthermore, water and copper are used as the materials for the fluid and electrodes, respectively.

In order to evaluate the changes in DEP force exerted on particles, one cut line across the top of the channel is drawn. As can be seen in Figure 2 and Figure 3, the variation of the forces across this line have been evaluated.

The electric current, electrical potential, and electrical field can be evaluated by solving the Ohm's law. Fundamental equations from Ohm's law are shown from equation (3) to equation (5).

$$\mathrm{E} = -\nabla \mathrm{V} \tag{3}$$

$$J = \sigma E + j\omega D \tag{4}$$

$$D = \varepsilon_0 \varepsilon_r E \tag{5}$$

J, σ, E, ω *and* V are electric current density, electrical conductivity, electrical filed, angular frequency, and electrical voltage, respectively. D is the corrected electrical field in different mediums, ε_0 is the relative permittivity of air and ε_r is the relative permittivity of the used medium. AC voltage is applied as an input, both real and imaginary terms are created in the electrical flux J and will be changed by the input frequency.

In this study, only the variable E is important as it has a direct influence on amount of DEP force, as demonstrated in equation (1). Furthermore, all other terms of equation (1) are constant for this specific study, except ∇E^2 term. Consequently, we focus on this term as it has a direct impact on the DEP force. The widths of electrode 1 and electrode 2 and also the width of the gap between the two electrodes. play a vital role on the magnitude and direction of the ∇E^2 term and the DEP force. Therefore, these parameters were used in this study.

IV. RESULTS AND DISCUSSION

As mentioned before, the parameter that affects the DEP force in Equation (1) is ∇E^2, which depends on the geometry of the device. The other parameters in this equation rely on the particle, medium, and frequency of the applied electric field. As for ∇E^2, only its horizontal component affects the lateral displacement of the particles. Thus, the horizontal component of ∇E^2 is used to optimize the electrodes geometry. As shown in Figure 2, the value of ∇E^2 is minimum on the top of the channel, resulting in the minimum DEP force. To make sure that all the particles are affected by DEP, the ∇E^2 term must be maximized on the top of the channel.

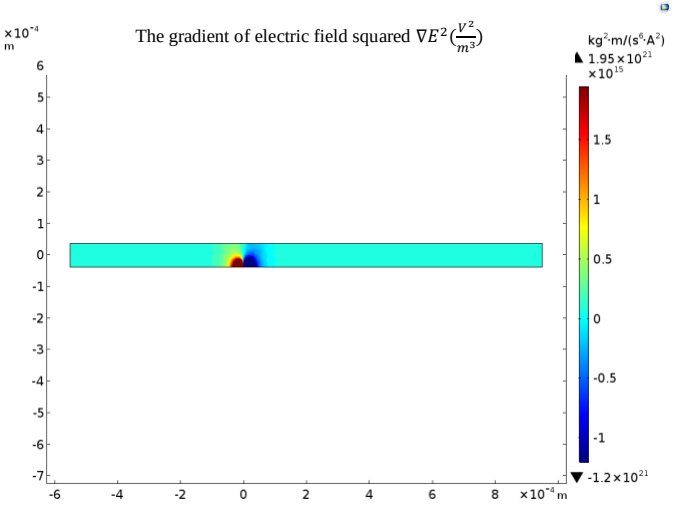

Figure 2. The contour of ∇E^2 inside a channel with the width of the electrodes of bot $W_1 = W_2 = 300$ µm and G= 5 µm.

First, the effect of the gap between the electordes is studied. For this, the electrodes are assumed to have the same size. Then, the gap is changed to find the optimum gap size resulting in the maximum value of ∇E^2 on the top of the channel. The curves in

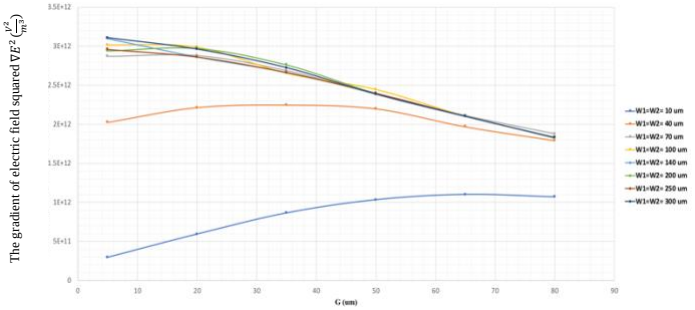

Figure 3. Maximum value of ∇E^2 along the top of the channel as a function of the gap size.

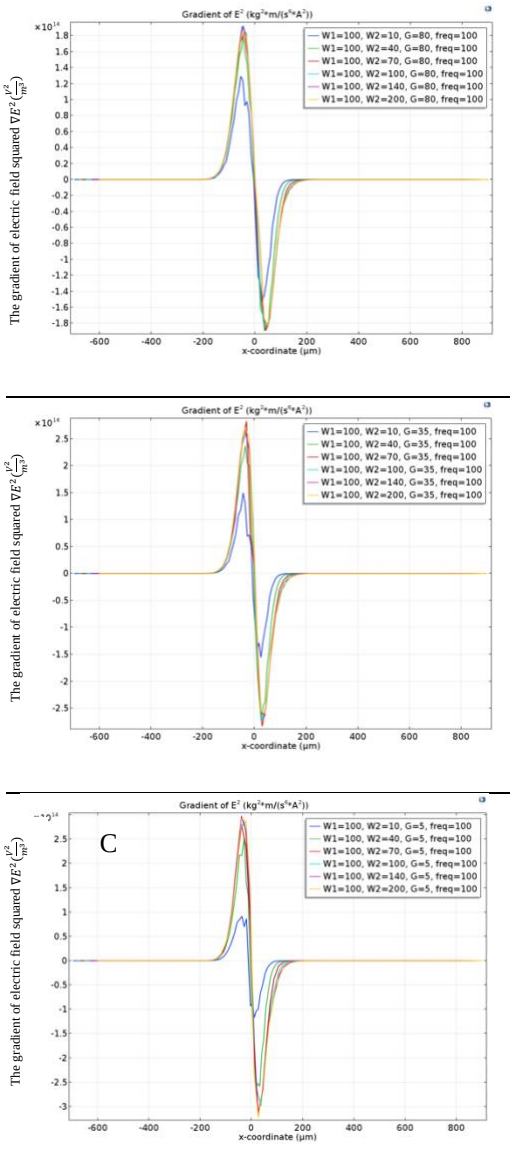

Figure 4. Variations of the exerted force on the particles as afucntion of the distance across the cut line. W_1 (th width of electrode 1) is considered as 10 μm while W_2 (the width of electrode 2) is varied from 10 to 200 μm. G (gap between two electrodes) is A) 80 μm , B) 35 μm and C) 5 μm.

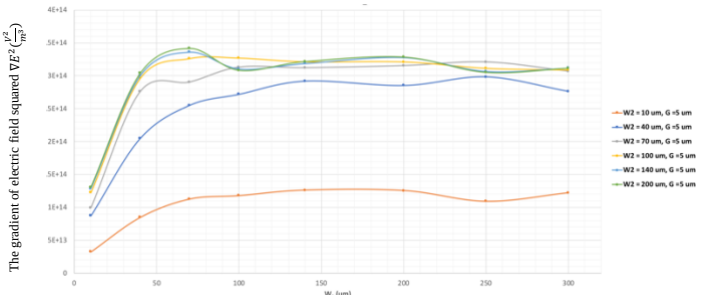

Figure 5. Maximum value of ∇E^2 on the top of the channel for the case that the gap is 5 μm and different combinations of the electrodes

Figure 3 are each associated with a certain value of the electrode width. The results show that all the curves have a similar trend (as the gap is reduced the value of ∇E^2 increases), except for the electrode widths of 10 and 40 μm. In order to make sure that this result is not just for the case of the same size electrodes, assuming that the first electrode is 100 μm wide, the second electrode's size is changed for three different gaps, and the results are provided in Figure 4. Comparing Figure 4 (A), (B) and (C) shows that even if the electrodes' sizes are not the same, as the gap decreases the DEP force increases. Hence, the optimum gap size is 5 μm.

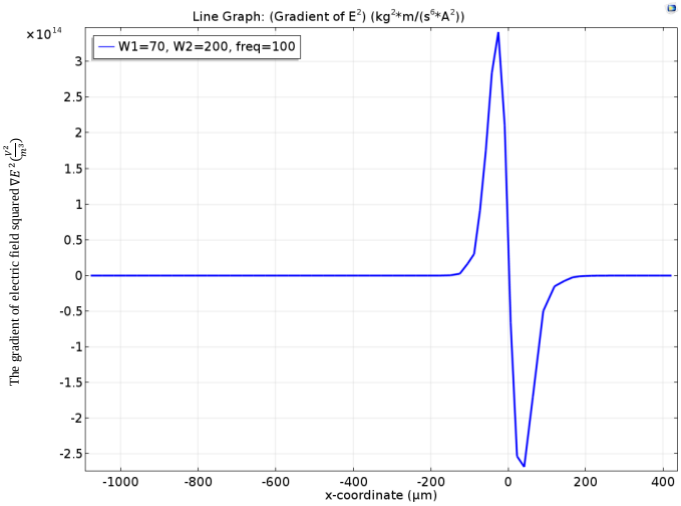

Figure 6. Variation of ∇E^2 along the top of the channel for a width of W1 = 70 μm and W2 = 200 μm and gap size of 5 μm.

To find the optimum electrode width, the simulation was run with the gap size of 5 μm and the electrode size combination of of 10 μm, 40 μm, 70 μm, 100 μm, 140 μm, 200 μm, 250 μm and 300 μm. The results in Figure 5 show that the electrodes smaller than 70 μm wide, lead to significantly lower ∇E^2. This means that electrodes smaller than 70 μm wide should be avoided in this design. However, increasing the width after 70 μm does not have a signigicant effect on ∇E^2. A closer look to the results shows that a slightly higher ∇E^2 (and DEP force) can be generated by using a combination of 70 μm and 200 μm wide electrodes.

With the optimum values of the gap and the electrode widths obtained, the variations in ∇E^2 are calculated and shown in Figure 6. This graph shows that the maximum value of the ∇E^2 term occurs on the side of the smaller electrode (blue line). Thus, the particle motion will be from the side of the large to the small electrodes. Based on these optimum values, the design shown in Figure 7 is used for a DEP-based micro-separator.

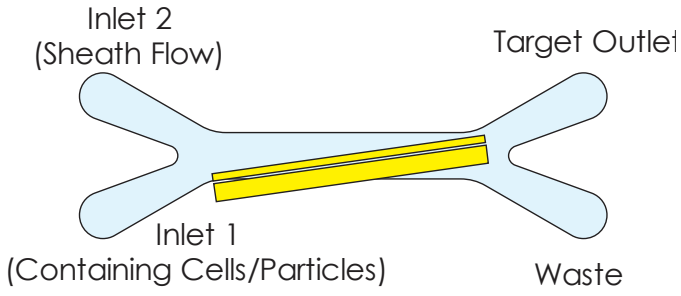

Figure 7. A schematic of the proposed DEP-based micro-seperator

V. CONCLUSIONS

In this study, COMSOL Multiphysics® tool was used to simulate the electric field created by two electrodes for a DEP-based cell/particle micro-separator. Different geometries in terms of the width of the electrodes and the gap between them have been investigated to find an optimum design, which leads to the maximum value of the DEP force on the top of the channel. The results show that in order to get the best outcome, the gap size must be as low as possible (which is 5 µm in our lab) and the width of the electrodes must be larger than 70 µm. Further investigation shows that the best results are obtained when the width of one of the electrodes is 75 µm and the other is 200 µm wide. Based on these results, a DEP-based micro-separator design is optimized.

REFERENCES

[1] B. Nestor, E. Samiei, R. Samanipour, A. Gupta, A. Van den Berg, M.D. de Leon Derby, Z. Wang, H.R. Nejad, K. Kim, M. Hoorfar, Digital microfluidic platform for dielectrophoretic patterning of cells encapsulated in hydrogel droplets, RSC Advances 6(62) (2016) 57409-57416.

[2] K. Park, S. Kabiri, S. Sonkusale, Dielectrophoretic lab-on-CMOS platform for trapping and manipulation of cells, Biomedical microdevices 18(1) (2016) 6.

[3] S.H. Kim, M. Antfolk, M. Kobayashi, S. Kaneda, T. Laurell, T. Fujii, Highly efficient single cell arraying by integrating acoustophoretic cell pre-concentration and dielectrophoretic cell trapping, Lab on a Chip 15(22) (2015) 4356-4363.

[4] Y.-C. Kung, D.L. Clemens, B.-Y. Lee, P.-Y. Chiou, Tunable dielectrophoresis for sheathless 3D focusing, Micro Electro Mechanical Systems (MEMS), 2015 28th IEEE International Conference on, IEEE, 2015, pp. 196-199.

[5] R. Wang, Y. Xu, H. Liu, J. Peng, J. Irudayaraj, F. Cui, An integrated microsystem with dielectrophoresis enrichment and impedance detection for detection of Escherichia coli, Biomedical microdevices 19(2) (2017) 34.

[6] A. Menachery, J. Burt, S. Chappell, R. Errington, D. Morris, P. Smith, M. Wiltshire, E. Furon, R. Pethig, Dielectrophoretic characterization and separation of metastatic variants of small cell lung cancer cells, Une 3 (2016) 386-389.

[7] J. Čemažar, T.A. Douglas, E.M. Schmelz, R.V. Davalos, Enhanced contactless dielectrophoresis enrichment and isolation platform via cell-scale microstructures, Biomicrofluidics 10(1) (2016) 014109.

[8] L. D'Amico, N.J. Ajami, J.A. Adachi, P. Gascoyne, J.F. Petrosino, Isolation and concentration of bacteria from blood using microfluidic membraneless dialysis and dielectrophoresis, Lab on a Chip 17(7) (2017) 1340-1348.

[9] B.J. Sanghavi, W. Varhue, A. Rohani, K.-T. Liao, L.A. Bazydlo, C.-F. Chou, N.S. Swami, Ultrafast immunoassays by coupling dielectrophoretic biomarker enrichment in nanoslit channel with electrochemical detection on graphene, Lab on a Chip 15(24) (2015) 4563-4570.

[10] V.V. Swaminathan, M.A. Shannon, R. Bashir, Enhanced sub-micron colloidal particle separation with interdigitated microelectrode arrays using mixed AC/DC dielectrophoretic scheme, Biomedical microdevices 17(2) (2015) 29.

[11] H. Zhu, X. Lin, Y. Su, H. Dong, J. Wu, Screen-printed microfluidic dielectrophoresis chip for cell separation, Biosensors and Bioelectronics 63 (2015) 371-378.

[12] S.H. Ling, Y.C. Lam, K.S. Chian, Continuous cell separation using dielectrophoresis through asymmetric and periodic microelectrode array, Analytical chemistry 84(15) (2012) 6463-6470.

[13] S. Li, M. Li, Y.S. Hui, W. Cao, W. Li, W. Wen, A novel method to construct 3D electrodes at the sidewall of microfluidic channel, Microfluidics and nanofluidics 14(3-4) (2013) 499-508.